TITLE:

Peel-1 negative selection promotes screening-free CRISPR-Cas9 genome editing in *Caenorhabditis elegans*.

AUTHORS:

Troy A. McDiarmid[1], Vinci Au[2], Donald G. Moerman[2], and Catharine H. Rankin[1,3*]

AFFILIATIONS:

[1]Djavad Mowafaghian Centre for Brain Health, University of British Columbia, 2211 Wesbrook Mall, Vancouver, British Columbia V6T 2B5, Canada
[2]Department of Zoology, Life Sciences Centre, University of British Columbia, 2350 Health Sciences Mall, Vancouver, British Columbia V6T 1Z4, Canada
[3]Department of Psychology, University of British Columbia, 2136 West Mall, Vancouver, British Columbia V6T 1Z4, Canada

Short title: *peel-1* negative selection CRISPR-Cas9 genome editing

***CORRESPONDING AUTHOR:**

Dr. Catharine Rankin
2136 West Mall,
Vancouver, BC
Canada, V6T 1Z4
604-822-5449
crankin@psych.ubc.ca

KEYWORDS:

CRISPR-Cas9, *peel-1* negative selection, *C. elegans*, homology-directed repair, genome editing

Abstract

Improved genome engineering methods that enable automation of large and precise edits are essential for systematic investigations of genome function. We adapted *peel-1* negative selection to an optimized Dual-Marker Selection (DMS) cassette protocol for CRISPR-Cas9 genome engineering in *Caenorhabditis elegans* and observed robust increases in multiple measures of efficiency that were consistent across injectors and four genomic loci. The use of Peel-1-DMS selection killed animals harboring transgenes as extrachromosomal arrays and spared genome edited integrants, often circumventing the need for visual screening to identify genome edited animals. To demonstrate the applicability of the approach, we created deletion alleles in the putative proteasomal subunit *pbs-1* and the uncharacterized gene *K04F10.3* and used machine vision to automatically characterize their phenotypic profiles, revealing homozygous essential and heterozygous behavioral phenotypes. These results provide a robust and scalable approach to rapidly generate and phenotype genome edited animals without the need for screening or scoring by eye.

Author summary

The ability to directly manipulate the genome and observe the resulting effects on the traits of an organism is a powerful approach to investigate gene function. CRISPR-based approaches to genome engineering have revolutionized such functional studies across model organisms but still face major challenges that limit the scope and complexity of projects that can be achieved in practice. Automating genome engineering and phenotyping would enable large-scale investigations of genome function in animals. Here, we describe the adaptation of *peel-1* negative selection to an optimized dual-marker selection cassette CRISPR-Cas9 genome engineering method in *C. elegans* and combine it with automated machine vision phenotyping to achieve functional studies without the need for screening or scoring by eye. To demonstrate the applicability of the approach, we generated novel deletion alleles in two understudied genes, *pbs-1* and *K04F10.3,* and used machine vision to characterize their phenotypic profiles, revealing homozygous lethal and heterozygous behavioral phenotypes. Our results open the door to systematic investigations of genome function in this model organism.

Introduction

Genome engineering – the ability to directly manipulate the genome, is a powerful approach to investigate its encoded functions. The nematode *Caenorhabditis elegans* has a rich history as a pioneering model system for the development of increasingly sophisticated methods to engineer the genome [1,2]. For decades, genome engineering in *C. elegans* relied on random mutagenesis to induce mutations or integrate transgenes, which often resulted in unwanted background mutations, transgene silencing, or overexpression [1,2]. The development of *Mos1* transposon-mediated Single Copy Insertion (MosSCI) and Deletion (mosDEL) finally allowed for deletion or insertion of designer sequences at a single copy into defined locations in the genome [1,3–6]. While immensely impactful, this method was limited in that it required the availability of a transposon at the edit site, preventing many edits from being made at the desired locus. Zinc finger and transcription activator-like nucleases offered more specificity but required considerable design effort for each new target, hindering their widespread adoption [7–9]. The discovery of CRISPR bacterial immune systems, followed promptly by their repurposing as a relatively easy to program RNA-guided system to target various effector domains (most notably the Cas9 nuclease) to precise locations in the genome revolutionized genome engineering across model systems [10–14]. In the short time since it's development, the versatility of CRISPR-based systems have allowed a remarkably diverse array of edits and modifications to be made in *C. elegans*, from single nucleotide variants and indels to larger deletions, insertions, direct replacements of entire genes and even programmed chromosomal rearrangements [2,9,15–27].

Despite these remarkable advances, CRISPR-based approaches for genome engineering in *C. elegans* still face major challenges that limit their efficiency and thus the scale and complexity of projects that can be achieved in practice. These can be broken down into issues that directly limit genome editing efficiency (e.g. the efficiency of Cas9 inducing a DNA double strand break or homology directed repair) or obstacles in screening that impede the identification and recovery of genome edited animals. Two major challenges in screening are that: 1) following microinjection of transgene DNA many of the F_1 progeny of injected P_0 adults will not be transgenic, and 2) even among transgenic animals, genome edited animals (or integrants) are

rare relative to the number of animals harboring transgenes as extrachromosomal arrays (referred to hereafter as 'arrays'). Both of these factors severely complicate the recovery of *bona fide* genome edited animals.

To begin to address these challenges, multiple selection schemes for CRISPR genome editing have been developed [1,2]. These include approaches based on editing of a secondary locus with a visible phenotype (e.g. co-CRISPR), or progressively more elaborate positive and negative selection schemes to enrich for animals where genome editing has occurred (reviewed in [2]). Two recent approaches coupled visual markers with drug resistance genes housed in Cre recombinase-excisable cassettes, allowing for drug selection against non-transgenic progeny [28,29]. These selection cassette methods effectively solved one of the major limitations of CRISPR genome editing in *C. elegans* by killing virtually all non-transgenic animals and provided a means to visually differentiate integrants from arrays, and thus represent the dominant methods for complex edits today. However, these approaches still face the limitation that animals harboring extrachromosomal arrays will also be resistant to drug selection and outnumber the desired integrants, necessitating cumbersome manual screening and isolation of putative genome edited animals. Thus, there is great need for an approach that simultaneously selects against both non-transgenics and arrays, leaving only genome edited animals.

PEEL-1 is a naturally occurring *C. elegans* sperm-derived toxin that is normally counteracted in the embryo by its antidote, ZEEL-1. Importantly, ectopic expression of *peel-1* at later life stages causes cell death and lethality [30]. This discovery motivated repurposing *peel-1* for array negative selection, in which a plasmid encoding heat shock driven *peel-1* is used to kill animals harboring arrays, thereby enriching for genome-edited integrants who have since lost the toxic array. Interestingly, while *peel-1* negative selection was developed as a component of MosSCI [4], and has been used in early CRISPR methods prior to the advent of excisable selection cassettes [20,26], it's use has faded in recent years.

Here, we integrate *peel-1* negative selection with an optimized CRISPR-Cas9 genome editing protocol for combined negative selection against both non-transgenics and arrays [25]. This scheme is built on the Dual-Marker Selection (DMS) cassette method [28], which does not

use heat shock driven cre-recombinase to excise it's selection cassette, making this approach compatible with heat shock driven *peel-1*. The combination of optimized guide selection, Cas9 RiboNucleoProtein (RNP) complexes, antibiotic selection for transgenics and *peel-1* negative selection against arrays effectively enriched for integrant animals to the point that they would often take over culture plates, allowing for screening-free genome editing. We then applied our approach to generate deletion alleles in putative proteasome subunit *pbs-1* and the uncharacterized gene *K04F10.3* to investigate the functional roles of these genes using machine vision. By combining our genome editing approach with automated machine vision phenotyping, we demonstrate the feasibility of generating and phenotyping genome edited animals without the need for manual screening or scoring, opening the door to systematic investigations of genome function.

Results

An optimized peel-1-DMS pipeline effectively kills arrays and spares genome-edited integrants

We used an optimized DMS genome editing strategy and guide selection tool (http://genome.sfu.ca/crispr/) to design programmed deletions at two separate loci, the uncharacterized genes *F53B6.7* and *F10E9.2* (**Fig 1A**) [25,28]. These deletions are predicted to result in null alleles. In the DMS strategy, application of the antibiotic Neomycin (G418) for drug selection 24h after injection kills virtually all non-transgenic F_1 progeny (**Fig 1B**). However, this scheme normally results in far more arrays than integrants, which can only be differentiated by the presence of body wall and pharyngeal muscle mCherry markers and/or the brightness/consistency of GFP fluorophore expression in the pharynx. While conceptually appealing, in practice the mCherry transgenes are often too dim to confidently visualize, leaving GFP as the only way to identify integrants, effectively reducing the process to searching for a dim needle in a variably bright haystack (**Fig 1B**). We hypothesized that the addition of *peel-1* negative selection to the optimized DMS pipeline (referred to hereafter as peel-1-DMS) delivered on the 5th day following injection would kill arrays without killing genome edited integrants, which by that point would have lost the toxic extrachromosomal array. Indeed, we observed that while

there were several integrants that had survived selection on days 7 and 8 post-injection, heat shock induction of *peel-1* killed arrays (**Fig 1C**).

Peel-1-DMS attenuates array-driven overpopulation/starvation and promotes screening-free genome editing at diverse loci

An important limitation of the standard DMS protocol is that worms carrying arrays crowd the culture plates, rapidly exhausting the food source and starving the population (**Fig 1C, top panel**). This prevents the rare integrants from surviving and reproducing, making screening more difficult. A single heat shock to induce *peel-1* negative selection decreased overpopulation-induced plate starvation approximately two-fold across two injectors each targeting the two *F53B6.7* and *F10E9.2* loci (**Fig 2A**). Although a potential concern might be that *peel-1* would also kill array-carrying integrants, effectively decreasing the editing efficiency/recovery of genome edited animals, we observed no differences in the efficiency (or total number of integrant animals retrieved) of CRISPR-Cas9 genome editing following *peel-1* treatment (**Fig 2B**). We also did not observe an increase in male progeny following *peel-1* induction (potentially because most animals that could be males would be arrays and have been killed off and/or a single 2h 34°C heat shock is insufficient to cause nondisjunction of the X chromosome and increase male proportions to a noticeable degree at a population level). Most importantly, the combined selection against arrays and reduced plate starvation allowed the integrants to win out, resulting in “pure” integrant plates and removing the need for any screening. We observed robust enrichment for pure integrant plates that was consistent across genomic loci (**Fig 2C**). Thus, through the addition of *peel-1* negative selection to an optimized DMS cassette method, *C. elegans* genome engineers can recover integrants from diverse loci without visual screening.

Peel-1-DMS is effective at two additional loci and multiple heat shock rounds further increases killing

While peel-1-DMS is highly effective at killing arrays, some animals do escape negative selection. However, animals that are not genome edited and managed to escape both *peel-1* and drug selection should still harbor the toxic *peel-1*-containing array, suggesting a testable

hypothesis that additional heat shock rounds to induce *peel-1* at later time points would further increase killing. To simultaneously test this hypothesis and validate our approach at additional target loci, we used peel-1-DMS to generate deletion alleles in two additional genes, the putative proteasome subunit *pbs-1* and the uncharacterized gene *K04F10.3*, and subjected animals to multiple heat shock rounds on either days 5 (standard), 5 & 7, or 5, 7, & 9. We then measured the strength of negative selection by scoring for signs of array-driven starvation 12 days post-injection. We did not observe increased selection with multiple heat shock rounds for *pbs-1*, as a single heat shock induction of *peel-1* on day 5 killed enough array carrying animals to prevent any signs of starvation for the entire 12-day testing period (**Fig 3A**). However, we did observe increased selection following multiple heat shock rounds for the *K04F10.3* target, indicating that while a single 2h heat shock at 5d is sufficient for effective selection, multiple heat shock rounds further increased killing using peel-1-DMS (**Fig 3B**). Thus, for both targets peel-1-DMS attenuated array overpopulation/plate starvation and simplified recovery of genome edited animals from integrant enriched plates. Taken together, these results demonstrate that peel-1-DMS is effective at multiple additional loci and that additional heat shock rounds can further strengthen *peel-1* negative selection.

Machine vision phenotypic profiles for novel deletion alleles of *pbs-1* and *K04F10.3* generated via peel-1-DMS

Peel-1-DMS allows for isolation of genome edited animals without the need for manual screening. If paired with automated phenotypic characterization, this would open to the door to full automation of diverse investigations of genome function in *C. elegans*. Toward this goal, we used our automated machine vision phenotyping system, the Multi-Worm Tracker (**Fig 4A**) [31] to generate phenotypic profiles for the *pbs-1* and *K04F10.3* deletion mutants we generated with peel-1-DMS. *pbs-1* was previously associated with a high-penetrance embryonic lethal phenotype in genome wide RNAi screens [32–34]. We confirm these knockdown results with precise CRISPR-Cas9 deletion alleles, ruling out compensation and definitively designating this gene as essential under standard laboratory growth conditions. Importantly, the DMS cassette does not use morphology or behavior altering selection markers and includes an easily visualized dominant pharyngeal GFP marker – allowing for simplified maintenance and

behavioral analysis of strains harboring heterozygous knockouts in essential genes, such as *pbs-1*.

High-throughput phenotypic profiling using the Multi-Worm Tracker revealed that *K04F10.3* mutant worms were shorter in length but not width, and displayed a more kinked body posture than wild-type worms (**Fig 4B-D**). (*K04F10.3* homozygous mutants displayed reduced fecundity but were still amenable to tracking). *pbs-1* heterozygotes, in contrast, displayed apparently normal morphology (**Fig 4B-D**) and initial locomotion speed (**Fig 4E**), and like *K04F10.3* mutants exhibited generally normal habituation of reversal responses to repeated mechanosensory stimulation (**S1 Fig**). Interestingly however, detailed behavioral analyses revealed that *pbs-1* heterozygotes were more easily aroused by touch than wild-type worms, observed as a prolonged increase in movement speed following repeated mechanosensory stimulation (**Fig 4E & F**). Taken together, these results demonstrate that combining peel-1-DMS with machine vision phenotyping allows for the generation and characterization of genome edited animals without the need for manual screening or scoring.

Discussion

We developed an integrated peel-1-DMS CRISPR-Cas9 genome editing strategy and observed robust increases in multiple measures of efficiency. Peel-1-DMS selection dramatically reduced the number of arrays without altering the number integrants. We demonstrated the broad applicability of the approach by generating four deletion alleles in different genes and phenotyping two of the deletion alleles in *pbs-1* and *K04F10.3*, revealing homozygous lethal and heterozygous behavioral phenotypes. Combining peel-1-DMS genome engineering with automated phenotypic characterization represents a streamlined strategy to precisely edit and functionally annotate the genome without any need for visual screening or scoring, opening the door for genome-wide knock-out and phenotyping efforts.

Peel-1 negative selection was developed as a key component MosSCI and improved the efficiency of the technique [1,4]. *Peel-1* negative selection was subsequently used in early laborious PCR screening-based CRISPR methods before the advent of excisable drug selection

cassettes, but it's use faded shortly after. There are several potential reasons for this, including incompatibility with the Self-Excising Cassette (SEC) CRISPR method that uses a heat shock inducible Cre recombinase to excise the selection cassette from the genome – meaning the heat shock used to induce *peel-1* would also destroy the repair template by excising the selectable markers prior to successful recovery of genome edited animals. Of note, *peel-1* selection has previously been suggested as a possible inclusion to the original DMS method by it's developers [28,35,36]. We demonstrate here that combining *peel-1* with an optimized sgRNA selection, homology-directed repair, and Cas9 RNP DMS approach yields increased efficiency. Indeed, the largest screening efficiency increases were observed with the most efficient guides, and are likely due to the combined use of *peel-1* with highly-effective Cas9 RNP complexes and optimized guide selection [19,25]. Importantly, our results suggest that the more efficient the editing of a particular locus is, the more likely it is that peel-1-DMS can drive the population to pure integrants.

Placing *peel-1* under an inducible promoter that does not require heat shock (e.g. a drug inducible promoter via further refinement of the Q system) [37,38] would make it compatible with SEC-based CRISPR engineering. This would also allow peel-1-DMS selection to be used when creating edits that result in heat sensitivity or other phenotypes incompatible with heat shock. Alternatively, given the speed of the current approach, the SEC constructs could simply be redesigned using the peel-1-DMS framework or used without heat shock (standard DMS screening) in the rare cases where target perturbation would cause severe heat sensitivity to the 2h 34°C exposure period.

Combined peel-1-DMS selection will be particularly useful for large-scale projects designed to repeatedly edit the same locus (e.g. creating large allelic series), as researchers will simply have to identify a guide efficient enough to ensure integrant enriched plates, bypassing the need for screening on each subsequent edit. Every guide RNA we designed with our selection tool resulted in >10% integrant enriched plates when tested with peel-1-DMS selection. Further, peel-1-DMS will reduce the need for new users to learn to distinguish arrays from integrants based on subtle fluorescence patterns. Even in the cases where screening is still required, researchers now only have to differentiate uneven array GFP from even integrant GFP

276 signal in a much smaller pool of animals, removing the need for access to multiple fluorescence
277 channels and making it physically easier to single integrants.
278
279 Peel-1-DMS selection provides the *C. elegans* community a robust, cheap, and easy to
280 implement method to increase the efficiency of diverse CRISPR-Cas9 genome engineering
281 projects. Our results and the rapid pace of CRISPR method development in *C. elegans* suggest
282 that recovering and functionally characterizing genome edited animals in a screening and
283 scoring-free manner may soon be the norm.
284
285
286 **Materials and Methods**

287 **Strains and maintenance**

288 Strains were maintained on NGM (nematode growth medium) plates seeded with the
289 *Escherichia coli* strain OP50 according to standard experimental procedures [39]. Strains were
290 maintained at 20°C unless otherwise noted. PD1074, the Moerman lab derivative of N2 [40],
291 was used for all CRISPR-Cas9 genome editing and behavioral experiments.

292 **CRISPR-Cas9 genome engineering**

293 The *C. elegans specific* guide RNA selection tool (http://genome.sfu.ca/crispr/) was used to
294 identify the F53B6.7, F10E9.2, *pbs-1*, and *K04F10.3* targeting crRNAs (dual guides for each
295 target). The complete list of crRNAs can be found in **S1 Table**.

296 Gene-specific crRNAs and universal tracrRNAs, both ordered from Integrated DNA
297 Technologies (IDT), were duplexed according to manufacturer's instructions then incubated with
298 purified Cas9 protein (kindly provided by the lab of Dr. Geraldine Seydoux, Johns Hopkins
299 University) to create RNPs for injection.

300 Homology directed repair constructs were designed and constructed according to the optimized
301 DMS protocol as previously described [25,28]. Briefly, homology arms flanking the region to be
302 deleted (450 bp homology with 50 bp adapter sequences for Gibson assembly) were ordered as

303 500 bp gBlocks from Integrated DNA Technologies (IDT). Repair template plasmids were
304 assembled using the NEBuilder Hifi DNA Assembly Kit (New England BioLabs) to incorporate
305 homology arms into the *loxP + Pmyo-2::GFP::unc-54 3'UTR + Prps-27::neoR::unc-54 3'UTR +*
306 *loxP* dual-marker selection cassette vector (provided by Dr. John Calarco).

307 Standard DMS injection mixes consisted of 2.5 ng/µl pCFJ90 (*Pmyo-2::mCherry*), 5 ng/µl
308 pCFJ104 (*Pmyo-3::mCherry*), 50 ng/µl gene-specific repair templates, and 0.5 µM gene-specific
309 Cas9 RNPs. Peel-1-DMS injection mixes were prepared the same except that they included
310 pMA122 (*Phsp16.41::peel-1*) at 10ng/µl for *peel-1* negative selection (**Fig 1A**). pCFJ90 - *Pmyo-*
311 *2::mCherry::unc-54utr* (Addgene plasmid # 19327 ; http://n2t.net/addgene:19327;
312 RRID:Addgene_19327), pCFJ104 - *Pmyo-3::mCherry::unc-54* (Addgene plasmid # 19328 ;
313 http://n2t.net/addgene:19328; RRID:Addgene_19328), and pMA122 - *peel-1* negative selection
314 (Addgene plasmid # 34873; http://n2t.net/addgene:34873; RRID:Addgene_34873) were gifts
315 from Dr. Erik Jorgensen.

316 Adult P_0 hermaphrodites were microinjected and then transferred in groups of 4 to standard
317 culture plates to recover [25,41]. 24h following microinjection 500µl of 25mg/ml G418 was added
318 to the culture plates for antibiotic selection (**Fig 1**).

319 ***Peel-1* induction**

320 Five days following microinjection, plates were transferred from 20°C incubation to a 34°C
321 incubator for a 2h heat shock to induce *peel-1.* For experiments involving multiple heat shocks
322 the same procedure was repeated on days 7 and 9.

323 **Screening and quantification**

324 Genome edited animals were identified by *peel-1* and/or G418 resistance, loss of
325 extrachromosomal array markers, and uniform dim fluorescence of the inserted GFP.

326 Experimenters blinded to condition scored plates for signs of starvation (exhausted OP50 food
327 source) at the indicated time points. Plates where virtually all animals (>95%) were putative

328 integrants based on *peel-1* and/or antibiotic resistance and visual markers were counted as
329 integrant enriched.

330 **Genotype confirmation**

331 Correct insertion of the DMS cassette sequence was confirmed by amplifying the two regions
332 spanning the upstream and downstream insertion borders using PCR. The genotyping strategy
333 is essentially as described for deletion allele generation via DMS cassette insertion in [25] and
334 [28].

335 Gene-specific forward primers were used with a universal reverse primer located within the GFP
336 coding region of the DMS cassette: CGAGAAGCATTGAACACCATAAC to amplify the upstream
337 insertion region for sequence confirmation.

338 Gene-specific reverse primers were used with a universal forward primer located within the
339 Neomycin resistance gene of the DMS cassette: CGAGAAGCATTGAACACCATAAC to amplify
340 the downstream insertion region for sequence confirmation.

341 Gene-specific wild-type primers were used in conjunction with either the forward or reverse
342 gene-specific primer to detect partial/imperfect edits or gene duplications.

343 The complete list of all gene-specific forward and reverse sequence confirmation primers can
344 be found in **S1 Table**.

345 **Strain list**

346 The following strains were generated by CRISPR-Cas9 genome engineering via microinjection
347 of plasmid DNA and Cas9 RNPs:

348 VC4544 *F53B6.7(gk5615[+LoxP Pmyo-2::GFP::unc-54 UTR Prps-27::NeoR::unc-54 UTR*
349 *LoxP+]) IV*

350 VC4352 *F10E9.2(gk5435[+LoxP Pmyo-2::GFP::unc-54 UTR prps-27::NeoR::unc-54 UTR*
351 *LoxP+]) I*

VC4353 *F10E9.2(gk5436[+LoxP Pmyo-2::GFP::unc-54 UTR prps-27::NeoR::unc-54 UTR LoxP+]) I*

VC4603 *pbs-1(gk5673[+LoxP Pmyo-2::GFP::unc-54 UTR Prps-27::NeoR::unc-54 UTR LoxP+]) IV*

VC4599 *K04F10.3(gk5669[+LoxP pmyo-2::GFP::unc-54 UTR prps-27::NeoR::unc-54 UTR LoxP+]) I*

Strains harboring programmed deletions in each of these four genes are available from the Caenorhabditis Genetics Center or upon request.

Behavioral assays

For the Multi-Worm Tracker mechanosensory habituation paradigm animals were synchronized for behavioral testing on NGM plates seeded with 50 µl of OP50 liquid culture 12-24 hours before use. For PD1074 wild-type controls and *pbs-1* heterozygous deletion mutants five gravid adults were picked to plates and allowed to lay eggs for 3-4 hours before removal. Due to reduced fecundity, *K04F10.3* homozygous mutants were age synchronized either by allowing 25 gravid adults to lay eggs for 3-4 hours before removal or by dissolving 25 gravid adults on the tracking plates in bleach to liberate their eggs. Both bleaching- and egg laying-based synchronization produced consistent results for all analyses and so were pooled to a single genotype group representing *K04F10.3* mutants. 72h old *pbs-1* heterozygous deletion mutant adults were identified via pharyngeal GFP (homozygous mutants are lethal while wild-type homozygotes do not carry GFP) and transferred to fresh Multi-Worm Tracker plates and tracked 24h later. For all Multi-Worm Tracker experiments 4-6 plates (20-100 worms/plate) were run for each strain. The animals were maintained in a 20°C incubator for 96 hours prior to testing [42].

Our behavioral paradigm consisted of a 5-minute period to recover from being placed on the tracker followed by a 5 min baseline period from which we computed multiple measures of morphology and baseline locomotion (**Fig 4E**) [42]. Beginning at 10 minutes we administered 30 mechanosensory stimuli to the Petri plate holding the animals at a 10 second interstimulus interval (ISI) using an automated push solenoid (**Fig 4A**). *C. elegans* respond to a

mechanosensory stimulus by emitting a reversal response (crawling backwards) allowing us to assess multiple measures of naïve sensitivity (e.g. reversal likelihood, duration, etc.; **S1 Fig**). With repeated stimulation there is a decrease in the likelihood of a reversal, as well as the duration, speed, and distance of reversals (habituation learning; **S1 Fig**). Following habituation training, we allowed a 5-minute recovery period after which we administered a 31st stimulus to gauge spontaneous recovery from short-term habituation - an assay of short-term memory retention [42].

Multi-Worm Tracker behavioral analysis and statistics

Multi-Worm Tracker software (version 1.2.0.2) was used for stimulus delivery and image acquisition. Phenotypic quantification with Choreography software (version 1.3.0_r103552) used "--shadowless", "--minimum-move-body 2", and "--minimum-time 20" filters to restrict the analysis to animals that moved at least 2 body lengths and were tracked for at least 20 s. Standard choreography output commands were used to output morphology and baseline locomotion features [31]. A complete description of the morphology, baseline locomotion, sensory, and habituation learning features can be found in the Multi-Worm Tracker user guide (https://sourceforge.net/projects/mwt/) [31]**.** The MeasureReversal plugin was used to identify reversals occurring within 1 s (d*t* = 1) of the mechanosensory stimulus onset. Comparisons of "final response" comprised the average of the final three stimuli. Arousal was defined as the increased mean absolute movement speed in the period following mechanosensory stimulation and prior to the delivery of the spontaneous recovery stimulus (**Fig 4E & F**; 600-1189 seconds). Custom R scripts organized and summarized Choreography output files [42]. No blinding was necessary because the Multi-Worm Tracker scores behavior objectively. Phenotypic features were pooled across plate replicates for each mutant strain and means were compared to the mean of the wild-type distribution with an unpaired t-test implemented using a linear model in R with a Benjamini-Hochberg control of the false discovery rate at 0.001 [42]. Sample sizes for each behavioral assay were chosen to be either equal to or greater than sample sizes reported in the literature that were sufficient to detect biologically relevant differences. Final figures were generated using the ggplot2 package in R [43].

All raw and processed data can be found at: (https://doi.org/10.5683/SP2/FVEEWE), All analysis code and the results of all statistical tests and are available at: (https://github.com/troymcdiarmid/peel-1).

Acknowledgements

We would like to thank Dr. John Calarco, Dr. Christian Frøkjær-Jensen, Dr. Geraldine Seydoux, Dr. Erik Jorgensen, and their labs for sharing constructs, reagents, and protocols or making them available. We would also like to thank members of the Rankin and Moerman labs for helpful discussions about the project.

Competing interests

None declared.

Data availability

All raw and processed data underlying the results presented in the study are available at: (https://doi.org/10.5683/SP2/FVEEWE), All analysis code and the results of all statistical tests and are available at: (https://github.com/troymcdiarmid/peel-1).

Strains and reagents are available from the CGC or upon request.

437 **REFERENCES:**

438

439 1. Nance J, Frøkjær-Jensen C. The caenorhabditis elegans transgenic toolbox. Genetics.
440 2019;212: 959–990. doi:10.1534/genetics.119.301506
441 2. Dickinson DJ, Goldstein B. CRISPR-Based Methods for Caenorhabditis elegans
442 Genome Engineering. Genetics. 2016;202: 885–901. doi:10.1534/genetics.115.182162
443 3. Frøkjær-Jensen C, Wayne Davis M, Hopkins CE, Newman BJ, Thummel JM, Olesen S-
444 P, et al. Single-copy insertion of transgenes in Caenorhabditis elegans. Nat Genet.
445 2008;40: 1375–1383. doi:10.1038/ng.248
446 4. Frøkjær-Jensen C, Davis MW, Ailion M, Jorgensen EM. Improved Mos1-mediated
447 transgenesis in C. elegans. Nat Methods. 2012;9: 117–8. doi:10.1038/nmeth.1865
448 5. Frøkjær-Jensen C, Davis MW, Sarov M, Taylor J, Flibotte S, LaBella M, et al. Random
449 and targeted transgene insertion in Caenorhabditis elegans using a modified Mos1
450 transposon. Nat Methods. 2014;11: 529–34. doi:10.1038/nmeth.2889
451 6. Robert V, Bessereau JL. Targeted engineering of the Caenorhabditis elegans genome
452 following Mos1-triggered chromosomal breaks. EMBO J. 2007;26: 170–183.
453 doi:10.1038/sj.emboj.7601463
454 7. Morton J, Davis MW, Jorgensen EM, Carroll D. Induction and repair of zinc-finger
455 nuclease-targeted double-strand breaks in Caenorhabditis elegans somatic cells. Proc
456 Natl Acad Sci U S A. 2006;103: 16370–16375. doi:10.1073/pnas.0605633103
457 8. Wood AJ, Lo TW, Zeitler B, Pickle CS, Ralston EJ, Lee AH, et al. Targeted genome
458 editing across species using ZFNs and TALENs. Science. 2011. p. 307.
459 doi:10.1126/science.1207773
460 9. Lo T-W, Pickle CS, Lin S, Ralston EJ, Gurling M, Schartner CM, et al. Precise and
461 heritable genome editing in evolutionarily diverse nematodes using TALENs and
462 CRISPR/Cas9 to engineer insertions and deletions. Genetics. 2013;195: 331–48.
463 doi:10.1534/genetics.113.155382
464 10. Jinek M, Chylinski K, Fonfara I, Hauer M, Doudna JA, Charpentier E. A programmable
465 dual-RNA-guided DNA endonuclease in adaptive bacterial immunity. Science. 2012;337:
466 816–21. doi:10.1126/science.1225829
467 11. Jiang W, Bikard D, Cox D, Zhang F, Marraffini LA. RNA-guided editing of bacterial

genomes using CRISPR-Cas systems. Nat Biotechnol. 2013;31: 233–239. doi:10.1038/nbt.2508

12. Cong L, Ran FA, Cox D, Lin S, Barretto R, Habib N, et al. Multiplex genome engineering using CRISPR/Cas systems. Science (80-). 2013;339: 819–823. doi:10.1126/science.1231143

13. Knott GJ, Doudna JA. CRISPR-Cas guides the future of genetic engineering. Science. American Association for the Advancement of Science; 2018. pp. 866–869. doi:10.1126/science.aat5011

14. Gasiunas G, Barrangou R, Horvath P, Siksnys V. Cas9-crRNA ribonucleoprotein complex mediates specific DNA cleavage for adaptive immunity in bacteria. Proc Natl Acad Sci U S A. 2012;109: E2579-86. doi:10.1073/pnas.1208507109

15. Waaijers S, Portegijs V, Kerver J, Lemmens BBLG, Tijsterman M, van den Heuvel S, et al. CRISPR/Cas9-targeted mutagenesis in Caenorhabditis elegans. Genetics. 2013;195: 1187–91. doi:10.1534/genetics.113.156299

16. Dejima K, Hori S, Iwata S, Suehiro Y, Yoshina S, Motohashi T, et al. An Aneuploidy-Free and Structurally Defined Balancer Chromosome Toolkit for Caenorhabditis elegans. Cell Rep. 2018;22: 232–241. doi:10.1016/j.celrep.2017.12.024

17. Chen X, Li M, Feng X, Guang S. Targeted Chromosomal Translocations and Essential Gene Knockout Using CRISPR/Cas9 Technology in Caenorhabditis elegans. Genetics. 2015;201: 1295–306. doi:10.1534/genetics.115.181883

18. Paix A, Schmidt H, Seydoux G. Cas9-assisted recombineering in C. elegans: genome editing using in vivo assembly of linear DNAs. Nucleic Acids Res. 2016;44: e128. doi:10.1093/nar/gkw502

19. Paix A, Folkmann A, Rasoloson D, Seydoux G. High efficiency, homology-directed genome editing in Caenorhabditis elegans using CRISPR-Cas9ribonucleoprotein complexes. Genetics. 2015;201: 47–54. doi:10.1534/genetics.115.179382

20. Dickinson DJ, Ward JD, Reiner DJ, Goldstein B. Engineering the Caenorhabditis elegans genome using Cas9-triggered homologous recombination. Nat Methods. 2013;10: 1028–1034. doi:10.1038/nmeth.2641

21. Friedland AE, Tzur YB, Esvelt KM, Colaiácovo MP, Church GM, Calarco JA. Heritable genome editing in C. elegans via a CRISPR-Cas9 system. Nat Methods. 2013;10: 741–

743. doi:10.1038/nmeth.2532

22. Chiu H, Schwartz HT, Antoshechkin I, Sternberg PW. Transgene-Free Genome Editing in *Caenorhabditis elegans* Using CRISPR-Cas. Genetics. 2013;195: 1167–1171. doi:10.1534/genetics.113.155879

23. Tzur YB, Friedland AE, Nadarajan S, Church GM, Calarco JA, Colaiácovo MP. Heritable custom genomic modifications in Caenorhabditis elegans via a CRISPR-Cas9 system. Genetics. 2013;195: 1181–5. doi:10.1534/genetics.113.156075

24. McDiarmid TA, Au V, Loewen AD, Liang J, Mizumoto K, Moerman DG, et al. CRISPR-Cas9 human gene replacement and phenomic characterization in *Caenorhabditis elegans* to understand the functional conservation of human genes and decipher variants of uncertain significance. Dis Model Mech. 2018;11: dmm036517. doi:10.1242/dmm.036517

25. Au V, Li-Leger E, Raymant G, Flibotte S, Chen G, Martin K, et al. CRISPR/Cas9 Methodology for the Generation of Knockout Deletions in *Caenorhabditis elegans*. G3; Genes|Genomes|Genetics. 2018; g3.200778.2018. doi:10.1534/g3.118.200778

26. Chen C, Fenk LA, de Bono M. Efficient genome editing in Caenorhabditis elegans by CRISPR-targeted homologous recombination. Nucleic Acids Res. 2013;41: e193. doi:10.1093/nar/gkt805

27. Katic I, Großhans H. Targeted heritable mutation and gene conversion by Cas9-CRISPR in Caenorhabditis elegans. Genetics. 2013;195: 1173–6. doi:10.1534/genetics.113.155754

28. Norris AD, Kim H-M, Colaiácovo MP, Calarco JA. Efficient Genome Editing in Caenorhabditis elegans with a Toolkit of Dual-Marker Selection Cassettes. Genetics. 2015;201.

29. Dickinson DJ, Pani AM, Heppert JK, Higgins CD, Goldstein B. Streamlined Genome Engineering with a Self-Excising Drug Selection Cassette. Genetics. 2015;200: 1035–1049. doi:10.1534/genetics.115.178335

30. Seidel HS, Ailion M, Li J, van Oudenaarden A, Rockman M V, Kruglyak L. A novel sperm-delivered toxin causes late-stage embryo lethality and transmission ratio distortion in C. elegans. PLoS Biol. 2011;9: e1001115. doi:10.1371/journal.pbio.1001115

31. Swierczek NA, Giles AC, Rankin CH, Kerr RA. High-throughput behavioral analysis in C.

elegans. Nat Methods. 2011;8: 592–8. doi:10.1038/nmeth.1625

32. Simmer F, Moorman C, van der Linden AM, Kuijk E, van den Berghe PVE, Kamath RS, et al. Genome-wide RNAi of C. elegans using the hypersensitive rrf-3 strain reveals novel gene functions. PLoS Biol. 2003;1: E12. doi:10.1371/journal.pbio.0000012

33. Takahashi M, Iwasaki H, Inoue H, Takahashi K. Reverse genetic analysis of the Caenorhabditis elegans 26S proteasome subunits by RNA interference. Biol Chem. 2002;383: 1263–6. doi:10.1515/BC.2002.140

34. Sönnichsen B, Koski LB, Walsh A, Marschall P, Neumann B, Brehm M, et al. Full-genome RNAi profiling of early embryogenesis in Caenorhabditis elegans. Nature. 2005;434: 462–9. doi:10.1038/nature03353

35. Kim H-M, Colaiácovo MP. CRISPR-Cas9-Guided Genome Engineering in C. elegans. Curr Protoc Mol Biol. 2016;115: 31.7.1-31.7.18. doi:10.1002/cpmb.7

36. Calarco JA, Friedland AE. Creating Genome Modifications in C. elegans Using the CRISPR/Cas9 System. Methods Mol Biol. 2015;1327: 59–74. doi:10.1007/978-1-4939-2842-2_6

37. Wei X, Potter CJ, Luo L, Shen K. Controlling gene expression with the Q repressible binary expression system in Caenorhabditis elegans. Nat Methods. 2012;9: 391–395. doi:10.1038/nmeth.1929

38. Monsalve GC, Yamamoto KR, Ward JD. A new tool for inducible gene expression in caenorhabditis elegans. Genetics. 2019;211: 419–430. doi:10.1534/genetics.118.301705

39. Brenner S. The genetics of Caenorhabditis elegans. Genetics. 1974;77: 71–94. Available: http://www.ncbi.nlm.nih.gov/pubmed/4366476

40. Yoshimura J, Ichikawa K, Shoura MJ, Artiles KL, Gabdank I, Wahba L, et al. Recompleting the Caenorhabditis elegans genome. Genome Res. 2019;29: 1009–1022. doi:10.1101/gr.244830.118

41. Mello C, Fire A. DNA Transformation. Methods Cell Biol. 1995;48: 451–482. doi:10.1016/S0091-679X(08)61399-0

42. McDiarmid TA, Belmadani M, Liang J, Meili F, Mathews EA, Mullen GP, et al. Systematic phenomics analysis of autism-associated genes reveals parallel networks underlying reversible impairments in habituation. Proc Natl Acad Sci U S A. 2020;117: 656–667. doi:10.1073/pnas.1912049116

43. Wickham H. Introduction. ggplot2. New York, NY: Springer New York; 2009. pp. 1–7. doi:10.1007/978-0-387-98141-3_1

Figure Legends

Fig 1. An optimized peel-1-DMS CRISPR-Cas9 genome editing pipeline kills arrays and spares genome edited integrants. (A) Schematic of the peel-1-DMS CRISPR-Cas9 genome editing method. Dual crRNAs targeting genes of interest are injected as RNPs in complex with Cas9 to induce double strand breaks. A homology-directed repair template is used to integrate a *myo-2::GFP* pharyngeal visual marker and a Neomycin resistance gene at the cut site for integrant positive selection. Co-injected extrachromosomal mCherry markers provide visual selection against arrays while *peel-1* negative selection kills animals harboring arrays. In the standard DMS method arrays are manually distinguished from arrays based on dimness/consistency of GFP expression in the pharynx. (B) Injection and selection protocols/experimental design to test the efficacy of peel-1-DMS selection compared to our previously reported DMS method. (C) Peel-1-DMS selection kills arrays while sparing genome-edited integrants. Images from the F53B6.7 experiment 7 days post-injection.

Fig 2. Peel-1-DMS attenuates array-driven overpopulation/starvation and promotes screening-free genome editing at diverse loci. (A) Proportion of injected plates showing signs of starvation with or without *peel-1* negative selection on the 7th day post-injection. Peel-1-DMS selection resulted in robust reductions in starvation across two injectors each targeting two distinct genomic loci. Note that “0%” indicates that no plates in that group showed signs of starvation. For the *F10E9.2* target, n = 6 plates for *peel-1* (+) and 6 plates for *peel-1* (-) for injector 1, and n = 8 plates for *peel-1* (+) and 16 plates for *peel-1* (-) for injector 2. For the *F53B6.7* target, n = 5 plates for *peel-1* (+) and 5 plates for *peel-1* (-) for injector 1, and n = 8 plates for *peel-1* (+) and 9 plates for *peel-1* (-) for injector 2. Note that each independent plate consists of 4 injected P_0 worms. (B) Peel-1-DMS selection did not alter the proportion of plates from which integrants were recovered (the number of plates per condition is the same as in panel A). (C) Proportion of plates enriched for integrant animals 11 (F10E9.2) or 12 (F53B6.7) days post-injection. For injector 1, n = 11 plates for *peel-1* (+) and 11 plates for *peel-1* (-). For injector 2, n = 25 plates for *peel-1* (+) and 16 plates for *peel-1* (-). Note that each independent plate consists of 4 injected P_0 worms. Peel-1-DMS selection robustly increased the proportion of integrant enriched plates.

Fig 3. Peel-1-DMS is effective at two additional loci and multiple heat shock rounds further increases killing. (A) Proportion of injected plates targeting *pbs-1* showing signs of starvation on the 12th day post-injection following one or multiple heat shock rounds to induce *peel-1*. (-) = no *peel-1* treatment, (+) = a single heat shock round on day 5, (++) = Two heat shock rounds on days 5 and 7, (+++) = three heat shock rounds on days 5, 7, and 9. Note that "0%" indicates that no plates in that group showed signs of starvation. (B) Proportion of injected plates targeting *K04F10.3* showing signs of starvation on the 12th day post-injection following multiple heat shock rounds to induce *peel-1*. (-) = no *peel-1* treatment, (+) = a single heat shock round on day 5, (++) = Two heat shock rounds on days 5 and 7, (+++) = three heat shock rounds on days 5, 7, and 9. N = 5 independent plates for all conditions. Note that each independent plate consists of 4 injected P_0 worms.

Fig 4. Deletion alleles of *pbs-1* and *K04F10.3* generated via peel-1-DMS selection reveal homozygous lethal and heterozygous behavioral phenotypes. (A) Schematic of the Multi-Worm Tracker machine vision phenotyping system. A high-resolution camera records a plate of worms while the Multi-Worm Tracker software creates comprehensive digital representations of the worms in real time from which multiple phenotypes are later computationally extracted offline. The Multi-Worm Tracker also coordinates delivery of stimuli, e.g. the mechanosensory stimuli delivered to the plates via a push solenoid used here. (B) Worm length across genotypes. Each dot represents the mean of an independent plate replicate. Each plate consists of 20-100 worms. (C) Worm width across genotypes. Each dot represents the mean of an independent plate replicate. Each plate consists of 20-100 worms. (D) The degree of body posture kink (in radians) across genotypes. Each dot represents the mean of an independent plate replicate. Each plate consists of 20-100 worms. (E) Mean absolute movement throughout the tracking session. *pbs-1* heterozygotes display initially normal locomotion speed and prolonged arousal following mechanosensory stimuli. (F) Quantification of aroused movement speed in the period following mechanosensory stimulation across genotypes. Each dot represents the mean of an independent plate replicate. Each plate consists of 20-100 worms. WT = PD1074 wild-type control, *K04F10.3* = *K04F10.3(gk5669)*, *pbs-1 +/-* = *pbs-1(gk5673)/+*.

Supporting information

S1 Fig. Habituation of reversal responses to mechanosensory stimuli in *K04F10.3* homozygous and *pbs-1* heterozygous deletion mutants. (A) Habituation of reversal probability across genotypes. (B) Habituation of reversal duration across genotypes. (C) Habituation of reversal speed across genotypes. Both *K04F10.3* homozygous and *pbs-1* heterozygous mutants displayed generally normal habituation (learned decrement) of reversal responses to repeated mechanosensory stimuli. Note that speed is consistently lower *K04F10.3* homozygous mutants, likely due to their reduced size (**Fig 4E**). Dots represent the mean of plate replicates (n = 4-6 plates per genotype). Each plate consists of 20-100 worms. Error bars represent standard error of the mean. WT = PD1074 wild-type control, *K04F10.3* = *K04F10.3(gk5669)*, *pbs-1 +/-* = *pbs-1(gk5673)/+*.

S1 Table. crRNA and PCR primer sequences.

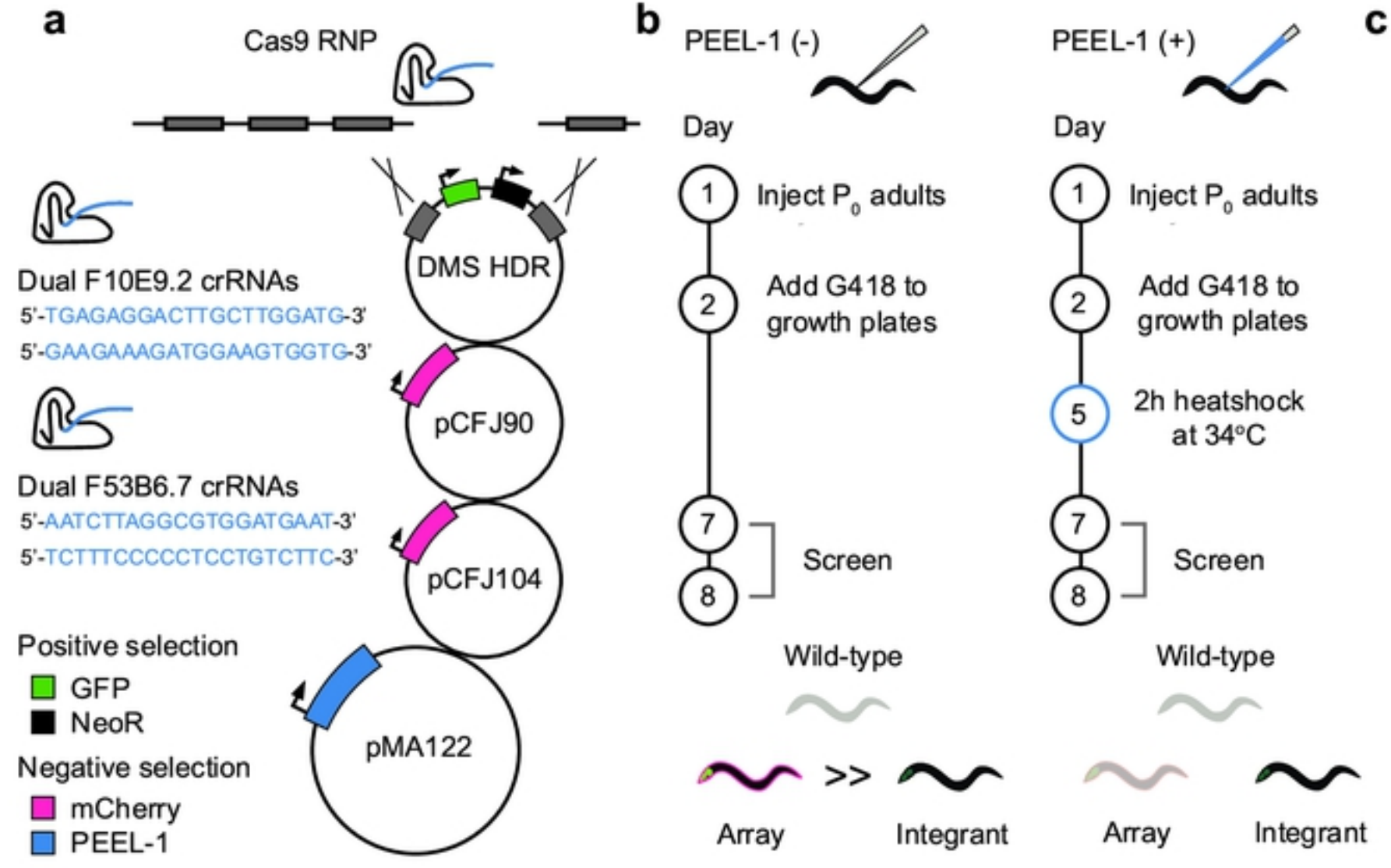
a
Cas9 RNP
DMS HDR
pCFJ90
pCFJ104
pMA122
Dual F10E9.2 crRNAs
5'-TGAGAGGACTTGCTTGGATG-3'
5'-GAAGAAAGATGGAAGTGGTG-3'
Dual F53B6.7 crRNAs
5'-AATCTTAGGCGTGGATGAAT-3'
5'-TCTTTCCCCCTCCTGTCTTC-3'
Positive selection
GFP
NeoR
Negative selection
mCherry
PEEL-1
b
PEEL-1 (-)
Day
1 Inject P0 adults
2 Add G418 to growth plates
7
8 Screen
Wild-type
Array
>>
Integrant
PEEL-1 (+)
Day
1 Inject P0 adults
2 Add G418 to growth plates
5 2h heatshock at 34°C
7
8 Screen
Wild-type
Array
Integrant
c
PEEL-1 (-)
PEEL-1 (+)

Figure 1

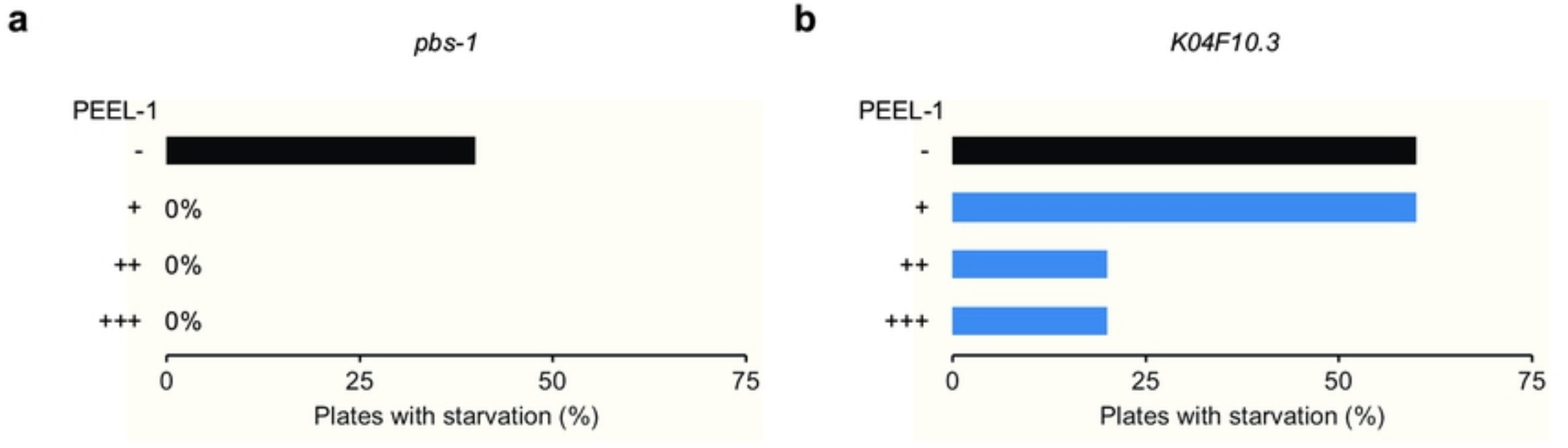
a
pbs-1
PEEL-1
-
+ 0%
++ 0%
+++ 0%
0
25
50
75
Plates with starvation (%)
b
K04F10.3
PEEL-1
-
+
++
+++
0
25
50
75
Plates with starvation (%)

Figure 3

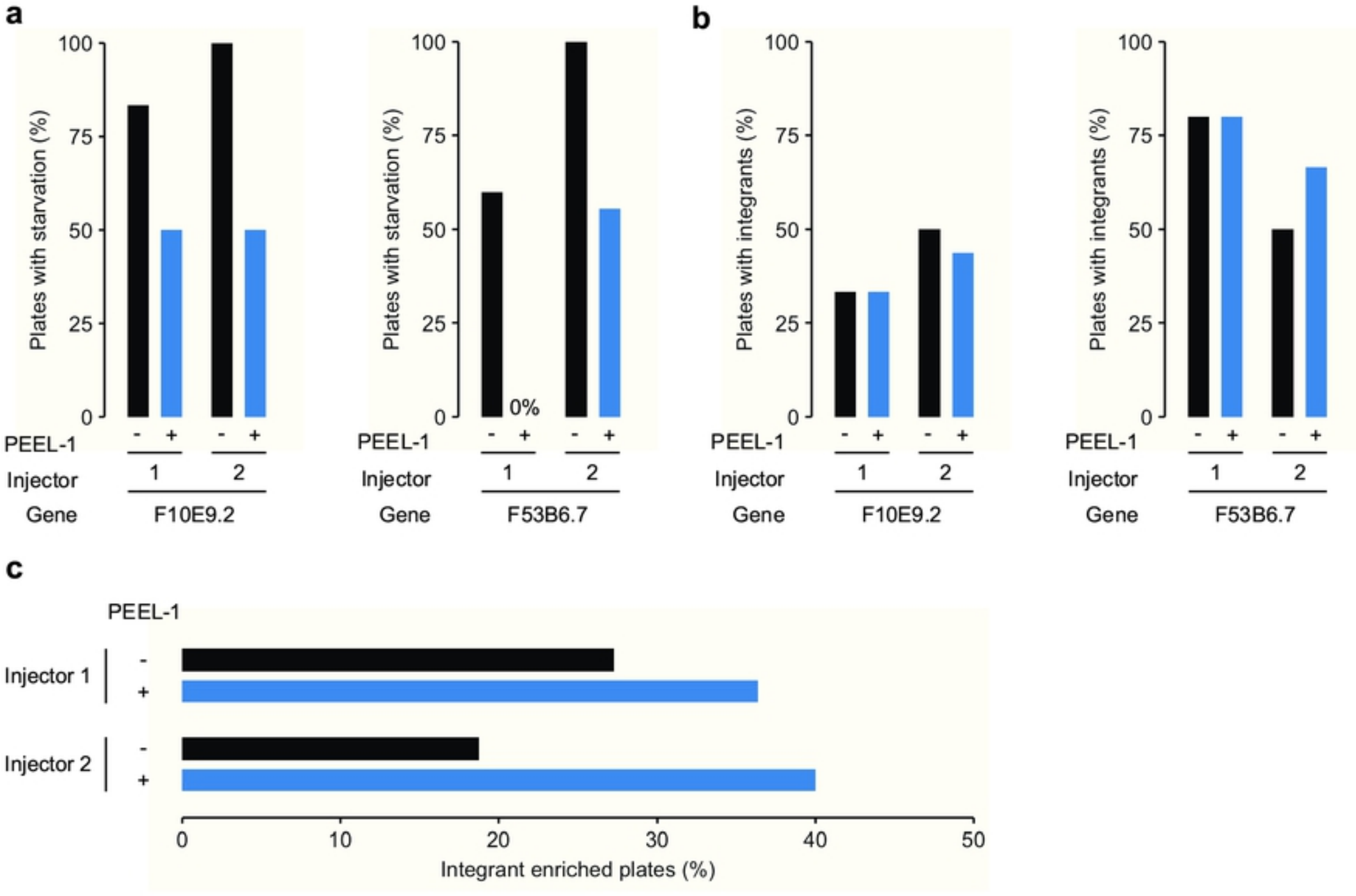
a
Plates with starvation (%)
100
75
50
25
0
PEEL-1
- + - +
Injector
1 2
Gene
F10E9.2
Plates with starvation (%)
0%
F53B6.7
b
Plates with integrants (%)
F10E9.2
F53B6.7
c
PEEL-1
Injector 1
Injector 2
0 10 20 30 40 50
Integrant enriched plates (%)

Figure 2

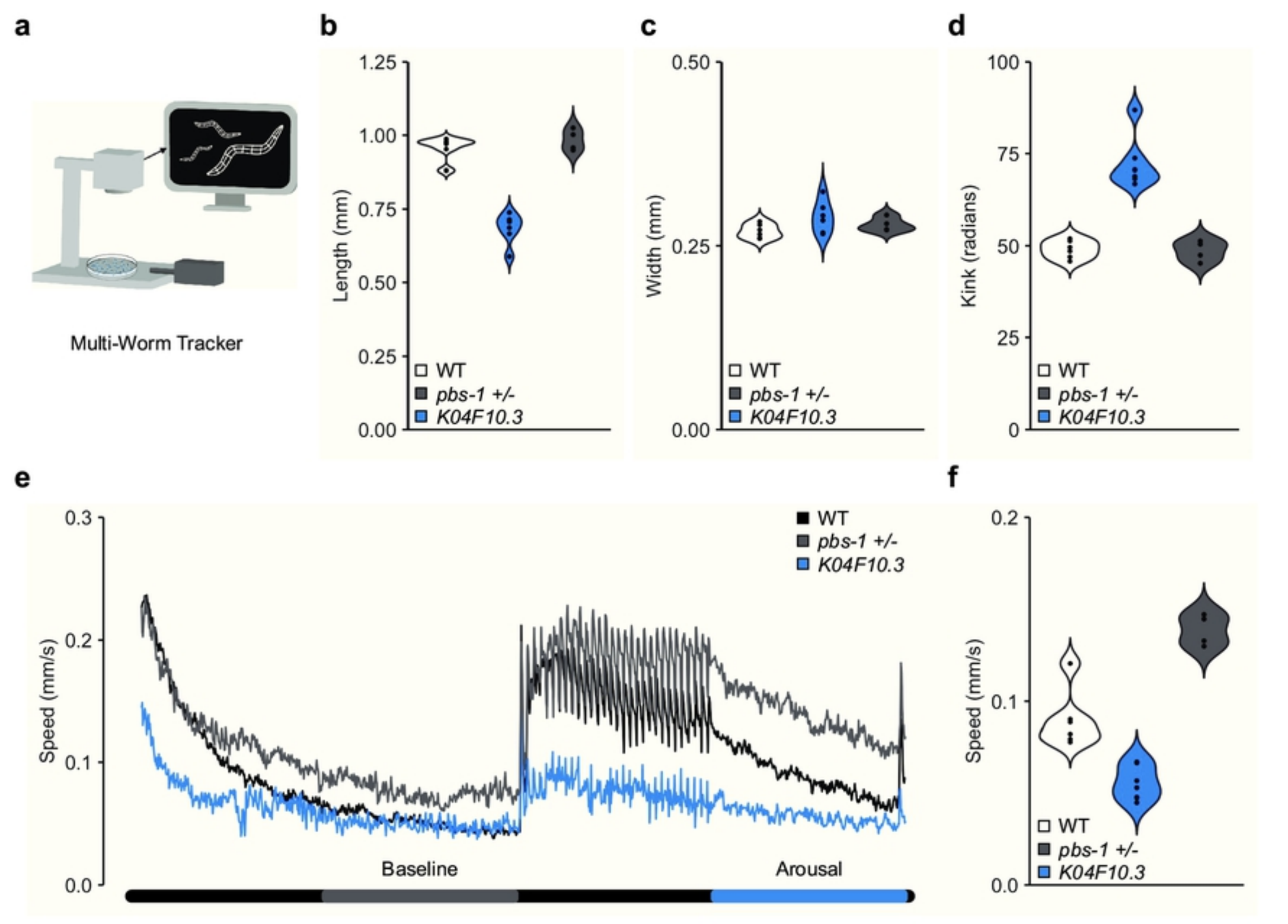
a
Multi-Worm Tracker
b
Length (mm)
1.25
1.00
0.75
0.50
0.25
0.00
WT
pbs-1 +/-
K04F10.3
c
Width (mm)
0.50
0.25
0.00
WT
pbs-1 +/-
K04F10.3
d
Kink (radians)
100
75
50
25
0
WT
pbs-1 +/-
K04F10.3
e
Speed (mm/s)
0.3
0.2
0.1
0.0
WT
pbs-1 +/-
K04F10.3
Baseline
Arousal
f
Speed (mm/s)
0.2
0.1
0.0
WT
pbs-1 +/-
K04F10.3

Figure 4